

# **Geometric Characterization of NACA Airfoils based on their Defining Parameters**

Tran Trung Nghia  
(Independent Study Project)

February 2026

## Abstract

Airfoil geometry is a fundamental determinant in aerodynamics, playing a crucial role in the performance, efficiency, and customized design of aircraft. The specific geometric characteristics of an airfoil directly influence its aerodynamic behavior, including lift, drag, and pitching moment coefficients. A clear understanding of basic airfoil design concepts is therefore essential for beginners in aerospace engineering. This article introduces the classical NACA airfoils and examines their geometric formulation using an Excel-based computational model.

Among the established airfoil families, the NACA 4-digit and 5-digit series, developed by the National Advisory Committee for Aeronautics (NACA), remain cornerstones in preliminary design, engineering education, and as benchmark profiles for advanced computational analyses. This report aims to provide students interested in aerospace engineering with a structured understanding of the NACA 4- and 5-digit airfoil nomenclature and the governing geometric parameters, thereby offering both visual and technical insight into how the specified digits determine the resulting airfoil shape.

# Introduction

Throughout the twentieth century, numerous airfoil families were introduced, including the Clark Y and the NACA 4-digit series. Over time, several thousand airfoils have been developed and experimentally tested. The Wright brothers themselves evaluated several hundred airfoils using a homemade wind tunnel, marking one of the earliest systematic investigations of wing profiles.

In the early years of aviation, aircraft wings relied heavily on external bracing systems, such as struts and wires, to provide structural support. As stronger construction materials became available, engineers sought to eliminate these external supports in order to reduce aerodynamic drag. Achieving this objective required thicker airfoil sections capable of providing sufficient structural strength, leading to the evolution of airfoil geometries similar to the Clark Y profile.

Early textbooks on flight theory frequently used the Clark Y airfoil to illustrate fundamental aerodynamic principles, and this practice has persisted over time. However, the airfoil families developed by the National Advisory Committee for Aeronautics (NACA) were documented more systematically. In particular, NACA Report No. 460, published in November 1933 and entitled *The Characteristics of the Seventy-Eight Related Airfoil Sections from Tests in the Variable Density Wind Tunnel*, provided detailed experimental data for a series of related airfoils.

As a governmental research agency, NACA conducted extensive wind tunnel testing to determine the aerodynamic efficiency of various airfoil configurations under different flight conditions. NACA later evolved into the National Aeronautics and Space Administration (NASA), which continued research and development in airfoil design. The resulting NACA airfoil profiles were designated using a standardized numbering system consisting of four, five, or six digits, enabling a direct relationship between numerical parameters and geometric characteristics.

# Airfoil Geometry

As early as the 1920s, research institutions in Europe and the United States began systematic measurements of the aerodynamic characteristics of airfoils in practical use. The results were organized into families of airfoils exhibiting specific aerodynamic properties. With a catalog of experimentally validated airfoils, aircraft designers were able to select suitable profiles efficiently for particular flight applications.

The National Advisory Committee for Aeronautics (NACA) conducted one of the most comprehensive and systematic investigations into the influence of airfoil geometry on aerodynamic performance. Early cambered airfoils, such as the Clark-Y and Göttingen sections, were known from initial wind tunnel experiments to exhibit favorable aerodynamic characteristics. NACA adopted these existing profiles as references; by removing the camber and normalizing the thickness-to-chord ratio,

the resulting geometries became systematically comparable. A polynomial curve fit was then used to define the thickness distribution, forming the foundation of many subsequent NACA airfoil families, including the classic NACA 00-series symmetric airfoils.

The airfoil geometry is defined in a Cartesian coordinate system in which the  $x$ -coordinate is measured along the chord line and normalized by the chord length  $c$ . The leading edge corresponds to  $x = 0$ , while the trailing edge corresponds to  $x = 1$ .

The airfoil surfaces are generated by superimposing the thickness distribution  $y_t(x)$  onto the mean camber line  $y_c(x)$ . The upper and lower surface coordinates are therefore defined as

$$\begin{aligned} x_u &= x - y_t \sin \theta, \\ y_u &= y_c + y_t \cos \theta, \end{aligned} \quad (1)$$

$$\begin{aligned} x_l &= x + y_t \sin \theta, \\ y_l &= y_c - y_t \cos \theta, \end{aligned} \quad (2)$$

where the local inclination angle  $\theta$  of the mean camber line is given by

$$\theta = \tan^{-1} \left( \frac{dy_c}{dx} \right). \quad (3)$$

## Formulation of Thickness Distributions

### Matching Empirical Curves by Simultaneous Power Equations

Many important developments in aerodynamics have historically been empirical in nature. As theoretical frameworks advanced, it became necessary to express these empirical observations in analytical form. Notable examples include the thickness equation of the classical NACA four-digit symmetric airfoils, thin-airfoil theory formulations, and spanwise loading distributions.

In addressing such problems, mathematicians rely primarily on two powerful analytical tools: power series expansions and Fourier series representations. These methods allow experimentally observed geometric or aerodynamic trends to be approximated using continuous mathematical expressions, mentioned in the reference [5].

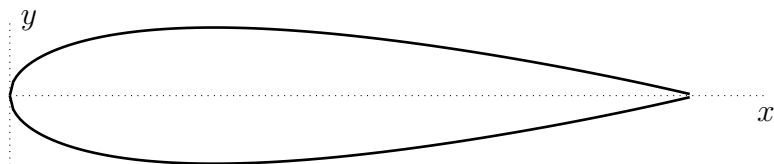


Figure 1: NACA 0020 profile

To illustrate this procedure, consider the development of the NACA 0020 airfoil equation. During the period from 1925 to 1935, two airfoils with markedly different camber characteristics were widely used: the Göttingen 398 and the Clark Y.

When the camber was removed from these profiles, their thickness distributions were found to be nearly identical. This observation motivated the adoption of a common thickness distribution combined with various parabolic camber lines in order to systematically investigate the influence of maximum camber magnitude and its chordwise location.

A critical step in this process was the formulation of a mathematical expression for the basic symmetric thickness shape. The empirical geometric data corresponded to a 20% thick airfoil defined in a Cartesian coordinate system, with the leading edge located at the origin and the trailing edge at  $x = 1$ .

The empirical conditions were:

1. Maximum ordinate

$$x = 0.3 \quad y = 1.0 \quad \frac{dy}{dx} = 0$$

2. Ordinate at trailing edge

$$x = 1.0 \quad y = 0.002$$

3. Trailing edge angle

$$x = 1.0 \quad \frac{dy}{dx} = -0.234$$

4. Nose shape

$$x = 0.1 \quad y = 0.078$$

Inspection of the nose region suggests that the leading-edge shape may be approximated by a square-root function of the form  $y = a_0\sqrt{x}$ . However, to ensure closure at the trailing edge, a linear correction term may be introduced as a first approximation. This leads to the preliminary form

$$y = a_0\sqrt{x} + a_1x.$$

To satisfy all five empirical conditions, higher-order polynomial terms are added, yielding the general expression

$$y = a_0\sqrt{x} + a_1x + a_2x^2 + a_3x^3 + a_4x^4.$$

Differentiation gives

$$\frac{dy}{dx} = \frac{1}{2}a_0x^{-1/2} + a_1 + 2a_2x + 3a_3x^2 + 4a_4x^3.$$

With five empirical constraints and five unknown coefficients, the resulting system of simultaneous equations can be solved to obtain

$$y = 0.2969\sqrt{x} - 0.1260x - 0.3516x^2 + 0.2843x^3 - 0.1015x^4.$$

For airfoils of other thickness ratios within the same family, the ordinates of the 0.20 thickness-ratio model are scaled by the factor  $(t/c)/0.20$ .

$$\pm y_t = \frac{t}{0.2} (0.2969\sqrt{x} - 0.1260x - 0.3516x^2 + 0.2843x^3 - 0.1015x^4)$$

The leading-edge radius is defined as the radius of curvature of the basic equation evaluated at  $x = 0$ . Owing to the presence of the term  $a_0\sqrt{x}$ , the radius of curvature remains finite at this point and can be shown to be  $a_0^2/2$ . Since the thickness scales linearly with the coefficients  $a_i$ , the leading-edge radius varies with the square of the thickness-to-chord ratio.

To define a symmetric airfoil in this family, the only required input is the desired thickness-to-chord ratio. These symmetric airfoils are designated by a four-digit number, for example NACA 0012, where the first two digits indicate zero camber and the last two digits specify the thickness-to-chord ratio in percent.

The leading-edge radius of this airfoil family is defined as the radius of curvature of the basic thickness equation evaluated at  $x = 0$ . Owing to the presence of the term  $a_0\sqrt{x}$ , the radius of curvature remains finite at the leading edge and can be shown to be

$$R_{LE} = \frac{a_0^2}{2} \left( \frac{t}{0.2} \right)^2 \equiv 1.019 t^2, \quad (4)$$

which is obtained by taking the limit as  $x \rightarrow 0$  of the standard expression for the radius of curvature,

$$R = \frac{\left[ 1 + \left( \frac{dy}{dx} \right)^2 \right]^{3/2}}{\left| \frac{d^2y}{dx^2} \right|}.$$

The trailing-edge angle is defined as the angle between the upper and lower surfaces at the trailing edge. It may be expressed as

$$\delta_{TE} = 2 \tan^{-1} \left[ \frac{t}{0.2} \left( \frac{a_0}{2} + a_1 + 2a_2 + 3a_3 + 4a_4 \right) \right] \equiv 2 \tan^{-1}(1.0625 t), \quad (5)$$

which is obtained by evaluating the slope of the thickness distribution at  $x = 1$  (or equivalently  $x = c$  in dimensional form).

The local surface inclination at the trailing edge is therefore

$$\varphi = \left| \frac{dy_t}{dx} \right|_{x=1}.$$

Because the upper and lower surfaces are symmetric with respect to the mean camber line for a symmetric airfoil, the total trailing-edge angle is twice this value, i.e.,  $\delta_{TE} = 2\varphi$ .

### Matching Empirical Curves by Simultaneous Fourier Series

A second approach for representing empirical aerodynamic curves employs trigonometric series consisting of sine and cosine terms. In many cases, this method is more efficient and mathematically convenient than using exponential relations.

Fourier series are particularly useful in aerodynamic theory because they allow complex distributions to be approximated by a finite number of harmonic terms. Two classical applications illustrate this approach.

The first application involves representing a camber line that is not symmetric about the mid-chord. In this case, a sine series is typically employed, since sine terms naturally satisfy boundary conditions at the leading and trailing edges while allowing asymmetric curvature.

The second application concerns the representation of lift distribution along a finite wing that is symmetric about the mid-span. In this case, a cosine series is commonly used, as cosine functions inherently capture symmetric distributions about the central axis.

By using simultaneous Fourier series, empirical aerodynamic curves can be matched with high accuracy while preserving essential physical boundary conditions. This approach forms an important theoretical foundation in thin airfoil theory and lifting-line theory.

### NACA 4-Digit Series

The first family of systematically developed airfoils was the NACA four-digit series. In this designation system, the first digit specifies the maximum camber of the mean camber line expressed as a percentage of the chord. The second digit indicates the chordwise location of the maximum camber in tenths of the chord measured from the leading edge. The final two digits represent the maximum thickness as a percentage of the chord [2].

For example, the NACA 2315 airfoil has a maximum mean camber of 2% of the

chord located at  $0.3c$  from the leading edge and a maximum thickness of 15% of the chord. Similarly, the NACA 0012 airfoil is symmetric and has a maximum thickness of 12% of the chord.

### Note on Symmetric Airfoils:

For a symmetric airfoil, the camber line coincides with the chord line. Consequently, the maximum camber is zero and its chordwise location is irrelevant. In this case, the first two digits (denoted by  $M$  and  $P$ ) are both zero, and the airfoil geometry is defined solely by the maximum thickness.

For example, NACA 0009 represents a symmetric airfoil with a maximum thickness equal to 9% of the chord.

### Mean Camber Line Formulation

The mean camber line of the four-digit series is defined by two parabolic segments of the general form [2]

$$y = b_0 + b_1x + b_2x^2.$$

The constants are determined from the following boundary conditions:

(1) *Camber-line endpoints*

$$\begin{aligned} x = 0, & \quad y = 0 \\ x = 1, & \quad y = 0 \end{aligned}$$

(2) *Maximum camber condition*

$$x = p, \quad y = m$$

Thus, the mean camber line is given by

$$y_c = \begin{cases} \frac{m}{p^2}(2px - x^2), & 0 \leq x \leq p \\ \frac{m}{(1-p)^2} [(1-2p) + 2px - x^2], & p \leq x \leq 1 \end{cases} \quad (6)$$

The slope of the camber line is obtained by differentiation:

$$\frac{dy_c}{dx} = \begin{cases} \frac{2m}{p^2}(p-x), & 0 \leq x \leq p \\ \frac{2m}{(1-p)^2}(p-x), & p \leq x \leq 1 \end{cases} \quad (7)$$

In practical applications, the parameters  $m$ ,  $p$ , and  $t$  may be varied to tailor the aerodynamic characteristics of the airfoil. Increasing the maximum camber generally enhances the lift coefficient, while the camber location influences the pitching moment and pressure distribution. The thickness ratio affects structural strength, drag characteristics, and leading-edge radius.

By systematically varying these parameters, a wide range of airfoils can be generated within the four-digit series to meet specific design requirements.

## NACA 5-Digit Series

The NACA five-digit airfoil series was developed by Jacobs and his associates following the success of the four-digit family. While the thickness distribution remained identical to that of the four-digit series, the mean camber line was substantially modified.

The primary objective of the new camber-line formulation was to position the maximum camber significantly farther forward along the chord. Experimental investigations had revealed that forward camber placement increased the maximum lift coefficient,  $C_{L_{\max}}$ . Accordingly, the five-digit series was designed to achieve:

- higher  $C_{L_{\max}}$ ,
- lower minimum drag  $C_{D_{\min}}$ ,
- reduced pitching moment.

A sub-family incorporating reflexed camber lines was also developed to produce approximately zero pitching moment about the quarter-chord. However, these reflexed sections have seen more limited practical use.

## Three-Digit Mean Camber Line

To obtain a camber line with a strongly forward maximum camber location, the so-called three-digit camber formulation was introduced in reference [4]-.

The camber line is defined in two regions such that the curvature (second derivative) decreases linearly to zero at a specified junction point  $x = m$  and remains zero from that point to the trailing edge.

Thus,

For  $0 \leq x \leq m$ :

$$\frac{d^2y}{dx^2} = k_1(x - m),$$

For  $m \leq x \leq 1$ :

$$\frac{d^2y}{dx^2} = 0.$$

The design constraints are:

(1) *Camber-line endpoints*

$$\begin{aligned} x = 0, & \quad y = 0, \\ x = 1, & \quad y = 0, \end{aligned}$$

(2) *Continuity at the junction point  $x = m$*

$$\begin{aligned} y_N &= y_T, \\ \left( \frac{dy}{dx} \right)_N &= \left( \frac{dy}{dx} \right)_T, \end{aligned}$$

where the subscripts  $N$  and  $T$  refer to the fore and aft equations, respectively.

The resulting camber line is

$$y_c = \begin{cases} \frac{k_1}{6} [x^3 - 3mx^2 + m^2(3-m)x], & 0 \leq x \leq m \\ \frac{k_1 m^3}{6} (1-x), & m \leq x \leq 1 \end{cases} \quad (8)$$

and the slope of the simple camber is

$$\frac{dy_c}{dx} = \begin{cases} \frac{k_1}{6} [3x^2 - 6mx + m^2(3-m)], & 0 \leq x \leq m \\ -\frac{k_1 m^3}{6}, & m \leq x \leq 1. \end{cases} \quad (9)$$

The parameter  $m$  was selected such that the maximum camber occurred at chordwise locations

$$p = 0.05P,$$

where  $P$  is the second digit of the five-digit designation. Thus, the standard locations are  $0.05c$ ,  $0.10c$ ,  $0.15c$ ,  $0.20c$ , and  $0.25c$ .

The location of maximum camber is obtained from the condition

$$\left. \frac{dy_c}{dx} \right|_{x=p} = 0,$$

which yields

$$p = m \left[ 1 - \sqrt{\frac{m}{3}} \right].$$

The constant  $k_1$  was then determined such that the design lift coefficient satisfied

$$C_{L_I} = 0.15L,$$

where  $L$  is the first digit of the NACA five-digit designation.

The tabulated parameters are as below

Camber-line designation	$p$	$m$	$k_1$
210	0.05	0.0580	361.400
220	0.10	0.1260	51.640
230	0.15	0.2025	15.957
240	0.20	0.2900	6.643
250	0.25	0.3910	3.230

Table 1: Tabulated parameters for non-reflexed NACA 5-digit camber lines ( $C_{L_I} = 0.3$ )

### Reflexed Mean Camber Line

To obtain zero pitching moment about the quarter-chord, a reflexed mean line was introduced. In this formulation, the curvature is again defined piecewise:

For  $0 \leq x \leq m$ :

$$\frac{d^2y}{dx^2} = k_1(x - m),$$

For  $m \leq x \leq 1$ :

$$\frac{d^2y}{dx^2} = k_2(x - m).$$

Solving the related equations yields

$$y_c = \begin{cases} \frac{k_1}{6} \left[ (x - r)^3 - \frac{k_2}{k_1} (1 - r)^3 x - r^3 x + r^3 \right], & 0 \leq x \leq r \\ \frac{k_1}{6} \left[ \frac{k_2}{k_1} (x - r)^3 - \frac{k_2}{k_1} (1 - r)^3 x - r^3 c + r^3 \right], & r \leq x \leq 1 \end{cases} \quad (10)$$

and the slope is derived using differentiation

$$\frac{dy_c}{dx} = \begin{cases} \frac{k_1}{6} \left[ 3(x - r)^2 - \frac{k_2}{k_1} (1 - r)^3 - r^3 \right], & 0 \leq x \leq r \\ \frac{k_1}{6} \left[ 3 \frac{k_2}{k_1} (x - r)^2 - \frac{k_2}{k_1} (1 - r)^3 - r^3 \right], & r \leq x \leq 1 \end{cases} \quad (11)$$

Imposing the condition of zero slope at the maximum camber location,

$$\left. \frac{dy_c}{dx} \right|_{x=p} = 0,$$

Camber-line designation	$p$	$m$	$k_1$	$k_2/k_1$
211	0.05	-	-	-
221	0.10	0.1300	51.990	0.000764
231	0.15	0.2170	15.793	0.00677
241	0.20	0.3180	6.520	0.0303
251	0.25	0.4410	3.191	0.1355

Table 2: Tabulated coefficients of reflex airfoil for  $C_{L_I} = 0.3$

leads to

$$\frac{k_2}{k_1} = \frac{3(m - p)^2 - m^3}{(1 - m)^3}.$$

For each prescribed value of  $p$ , the parameter  $m$  was determined to satisfy the condition of zero quarter-chord pitching moment ( $C_{m_{c/4}} = 0$ ). Subsequently,  $k_1$  was evaluated to produce a design lift coefficient of

$$C_{L_I} = 0.3.$$

The tabulated values of  $m$ ,  $k_1$ , and  $k_2/k_1$  are summarized above.

In practical design applications, the defining parameters of the five-digit series are not restricted to the tabulated integer values. Instead, they may be treated as continuous variables to achieve specific aerodynamic requirements.

By adjusting the camber magnitude, camber location, and thickness ratio, designers can tailor the lift characteristics, pitching moment behavior, and drag performance to meet particular mission profiles.

Thus, although originally defined by discrete designations, the five-digit formulation provides a flexible analytical framework for systematic airfoil development.

## NACA 4- and 5-Digit Modified Series

The modified NACA four- and five-digit airfoil families were developed to provide greater geometric flexibility while preserving the basic thickness characteristics of the original series.

In the modified designation, the airfoil number is followed by a dash and a two-digit suffix (e.g., NACA 0012-63). The first digit after the dash represents the leading-edge radius index, and the second digit indicates the location of maximum thickness in tenths of the chord measured from the leading edge [6].

## Thickness Distribution

The thickness distribution is defined piecewise so that the leading-edge radius and the chordwise location of maximum thickness may be varied independently.

If the chord is taken the position  $x$  axis from 0 to 1, the ordinates  $y$  from the leading edge to the maximum thickness location ( $0 \leq x \leq m$ ),

$$\pm y_t = a_0\sqrt{x} + a_1x + a_2x^2 + a_3x^3,$$

From the maximum thickness location to the trailing edge ( $m \leq x \leq 1$ ),

$$\pm y_t = d_0 + d_1(1-x) + d_2(1-x)^2 + d_3(1-x)^3.$$

The constants are determined from the following geometric constraints:

1. Specified maximum thickness

$$x = m \quad y = 0.10 \quad \frac{dy}{dx} = 0$$

2. Prescribed leading-edge radius

$$x = 0 \quad R = \frac{a_0^2}{2}$$

3. Specified radius of curvature at the point of maximum thickness

$$x = m \quad R = \frac{(1-m)^2}{2d_1(1-m) - 0.588}$$

4. Specified trailing-edge ordinate

$$x = 1 \quad y = d_0 = 0.002$$

5. Prescribed trailing-edge angle

$$x = 1 \quad \frac{dy}{dx} = d_1 = f(m)$$

These conditions ensure continuity of ordinate, slope, and curvature at the junction point  $x = m$ .

## Leading-Edge Radius Index

The leading-edge index  $I$  controls the magnitude of the leading-edge radius and is proportional to the coefficient  $a_0$ .

The relationship between the leading-edge radius  $R_{LE}$  and the index number  $I$  is given by

$m$	$d_1$
0.2	0.200
0.3	0.234
0.4	0.315
0.5	0.465
0.6	0.700

Table 3: Selected values of  $d_1$  to prevent curvature reversal [6]

$$R_{LE} = \frac{1}{2} \left( 0.2969 \frac{t}{0.2} \frac{I}{6} \right)^2.$$

Type	Leading-edge Index $I$	$a_0$
Sharp	0	0
Quarter-normal	3	0.148450
Normal	6	0.296900
Three-times normal	9	0.514246

Table 4: Leading-edge index classification

As in the original four-digit series, the ordinates vary linearly with the thickness–chord ratio.

Thus, for any desired thickness ratio  $t/c$ , the ordinates are obtained by scaling the design thickness distribution proportionally.

The original NACA four-digit series is a special case of the modified formulation corresponding to:

- Leading-edge index  $I = 6$  (normal leading edge),
- Maximum thickness location at 0.30c.

Hence, the classical four-digit airfoil can be interpreted as a particular instance of the more general modified family.

### Modified Five-Digit Series

The modified five-digit airfoils retain the same camber-line definitions as the standard five-digit series but incorporate the modified thickness formulation described above.

Thus, the camber line is defined according to the five-digit design equations, while the thickness distribution is replaced by the modified polynomial expressions that allow independent control of:

- Leading-edge radius,
- Maximum thickness location,
- Trailing-edge angle.

This combination provides increased flexibility in tailoring airfoil geometry for specific aerodynamic performance requirements.

In practical aerodynamic design, the modified formulation allows the defining parameters to be treated as continuous variables rather than discrete tabulated values.

By adjusting the camber magnitude, camber location, thickness ratio, leading-edge radius, and maximum thickness position, designers can systematically optimize lift characteristics, drag performance, and pitching moment behavior.

Consequently, the modified NACA families provide a versatile analytical framework for preliminary airfoil design.

## NACA 1-Series Airfoils and 16-Series Designation

Unlike the previously discussed airfoil families, which were defined primarily through geometric relationships, the NACA 1-Series airfoils were developed using inverse airfoil design methods based on aerodynamic theory. By the late 1930s, significant advances had been made in understanding the relationship between pressure distribution and airfoil performance. Instead of prescribing the airfoil geometry directly, the design process began by specifying a desired pressure distribution along the airfoil surface. This pressure distribution determines the lift characteristics, drag properties, and stall behavior. The corresponding airfoil geometry was then derived mathematically to produce the prescribed pressure distribution.

As a result, the 1-Series airfoils were not generated using simple analytical polynomial expressions like the Four- or Five-Digit Series. Rather, their geometry was obtained numerically from aerodynamic design criteria. The characteristics of the 1-series airfoil were studied in the reference [3].

The NACA 1-Series airfoils are identified using a five-digit designation, as illustrated by the example NACA 16-212. The designation is interpreted as follows:

- The first digit, “1”, identifies the airfoil as belonging to the 1-Series, which was designed using inverse methods to achieve favorable pressure distributions and improved high-speed aerodynamic performance.
- The second digit indicates the chordwise location of minimum pressure in tenths of the chord from the leading edge. In the designation 16-212, the value “6” indicates that the minimum pressure occurs at  $0.6c$ , or 60% of the chord.

- The first digit following the dash specifies the design lift coefficient in tenths. In this example, the digit “2” corresponds to a design lift coefficient of

$$C_{L,design} = 0.2$$

- The final two digits indicate the maximum thickness in percent of the chord. In this case, “12” corresponds to a thickness ratio of

$$\frac{t}{c} = 0.12$$

The NACA 16-Series airfoils represent the most widely used subset of the 1-Series. These airfoils were specifically designed to maintain favorable pressure gradients over a large portion of the chord, thereby reducing drag and delaying boundary layer separation. Compared with earlier airfoil families, the minimum pressure point is located farther aft, which reduces the magnitude of the suction peak near the leading edge and improves performance at moderate to high speeds.

Geometrically, the thickness distribution of the 16-Series airfoils is similar to that of the modified four-digit series, typically with a leading-edge radius index near 4 and a maximum thickness location near 50% of the chord, presented in the reference [1] and studied aerodynamic characteristics were reported in reference [6]. However, unlike the purely geometric four-digit and five-digit families, the camber and overall shape of the 16-Series airfoils are determined primarily by aerodynamic performance requirements, particularly the specified design lift coefficient.

Because the NACA 16-Series airfoils are the only members of the 1-Series that have seen widespread practical application, the family is commonly referred to simply as the NACA 16-Series rather than as part of the broader 1-Series classification.

## NACA 6-Series and 6A-Series Airfoils

Although NACA experimented with approximate theoretical methods in developing the 2-Series through the 5-Series airfoils, these approaches were not sufficient to accurately produce the desired pressure distributions and drag characteristics. Consequently, a more rigorous theoretical method was developed, leading to the NACA 6-Series airfoils. Similar to the earlier 1-Series, the 6-Series airfoils were designed using inverse airfoil theory, in which the desired pressure distribution was specified first, and the airfoil geometry was then mathematically derived to produce that distribution.

The primary objective of the 6-Series airfoils was to maximize the extent of laminar flow over the airfoil surface. By maintaining laminar boundary layer flow over a substantial portion of the chord, the skin-friction drag could be significantly reduced within a specified range of lift coefficients. This resulted in a characteristic “low-drag bucket,” in which the drag coefficient remains low over a finite range of lift conditions.

The designation system for the NACA 6-Series airfoils is more complex than that of earlier families due to the inclusion of parameters related to pressure distribution and aerodynamic performance. A representative example is the NACA 641-212 airfoil with  $a = 0.6$ . The designation is interpreted as follows:

- The first digit, “6”, identifies the airfoil as belonging to the 6-Series, indicating that it was designed to achieve extended regions of laminar flow and reduced drag.
- The second digit specifies the chordwise location of minimum pressure in tenths of the chord from the leading edge. In this case, “4” indicates that the minimum pressure occurs at  $0.4c$ .
- The subscript digit, “1”, defines the range of lift coefficients over which low drag is maintained. Specifically, it indicates that the low-drag region extends over a range of  $\pm 0.1$  about the design lift coefficient.
- The first digit following the dash specifies the design lift coefficient in tenths. Here, “2” corresponds to

$$C_{L,design} = 0.2$$

- The final two digits specify the maximum thickness as a percentage of the chord. In this example,

$$\frac{t}{c} = 0.12$$

- The parameter  $a$  specifies the fraction of the chord over which the favorable pressure gradient is maintained on the upper surface. For  $a = 0.6$ , the favorable pressure gradient extends over 60% of the chord. If not specified,  $a$  is typically assumed to be 1.0.

## Camber Line

Unlike the four-digit and five-digit airfoil families, the camber line of the NACA 6-Series airfoils is not defined using simple polynomial expressions. Instead, the camber line is determined using inverse aerodynamic design methods to achieve the specified pressure distribution corresponding to the desired design lift coefficient. The camber distribution is calculated numerically using thin airfoil theory and potential flow analysis.

The mean lines commonly used with the NACA 6-series airfoils produce a uniform chordwise loading from the leading edge to the point  $x = a$  and a linearly decreasing load from this point to the trailing edge. Data for NACA mean lines with values of  $a$  equal to 0, 0.1, 0.2, 0.3, 0.4, 0.5, 0.6, 0.7, 0.8, 0.9, and 1.0 are presented in the supplementary figures. The ordinates were computed by the following formula,

which represents a simplification of the original expression for mean-line ordinates given in reference [3]:

$$y = \frac{c_{l_i}}{2\pi(A+1)} \left\{ \frac{1}{1-A} \left[ \frac{1}{2}(A-x)^2 \ln(A-x) - \frac{1}{2}(1-x)^2 \ln(1-x) + \frac{1}{4}(1-x)^2 - \frac{1}{4}(A-x)^2 \right] - x \ln x + g - hx \right\}$$

where

$$g = -\frac{1}{1-A} \left[ A^2 \left( \frac{1}{2} \log_e A + \frac{1}{4} \right) + \frac{1}{4} \right]$$

$$h = \frac{1}{1-A} \left[ \frac{1}{2}(1-A)^2 \log_e(1-A) - \frac{1}{4}(1-A)^2 \right] + g$$

## Thickness Distributions

Similarly, the thickness distribution of the NACA 6-series airfoils was derived using theoretical aerodynamic methods rather than empirical geometric fitting. The design procedure was based on potential flow theory and conformal mapping techniques from complex analysis to generate airfoil shapes capable of producing prescribed pressure distributions. The derivation methods are introduced in [3], and a detailed theoretical analysis is presented in [5].

The mathematical foundation of this design approach relies on conformal transformation techniques, which enable the mapping of simple analytical flow solutions into airfoil geometries with specific aerodynamic characteristics. These transformations preserve the governing equations of inviscid, irrotational flow while reshaping the geometry. As a result, they allow designers to control pressure gradients, ensure smooth pressure recovery, and promote extended laminar flow over a significant portion of the airfoil surface.

One of the classical derivation methods in thin airfoil theory is the Joukowski transformation, a conformal mapping used to generate the Joukowski airfoil from a circular cylinder in the complex plane. Although the NACA 6-series airfoils are not simple Joukowski profiles, the theoretical framework is conceptually similar. Conformal mapping techniques provide the analytical basis for determining thickness distributions that correspond to specified pressure distributions.

## NACA 6A-Series

The NACA 6A-Series airfoils represent a modified version of the original 6-Series. The principal modification was the adjustment of the mean camber line to provide improved pitching moment characteristics, particularly for applications requiring reduced sensitivity of the pitching moment to lift coefficient. This was achieved by modifying the camber distribution while retaining the favorable laminar flow characteristics of the original 6-Series airfoils.

The 6A-Series airfoils were particularly useful in applications requiring improved longitudinal stability, such as propeller sections and certain aircraft wing designs.

Because of their superior drag characteristics within the design lift range, the NACA 6-Series and 6A-Series airfoils became widely used in high-performance aircraft and continue to serve as important reference airfoils in aerodynamic design.

## Methodology

### Excel Graph (2D)

Microsoft Excel is one of the simplest tools for generating graphs and calculating tabulated data. This approach is particularly useful for understanding preliminary concepts in aircraft design, especially wing profiles, which are fundamental components of an airplane.

Using cosine spacing with 1000 points provides an efficient method for distributing coordinates along the chord. The primary advantage of cosine spacing is its ability to increase the density of points in regions with high curvature, thereby producing a smoother and more accurate airfoil representation.

There are two commonly used cosine spacing methods:

- (1) The  $x$ -coordinates are defined using a sequence of angles ranging from 0 to  $\frac{\pi}{2}$ . This method concentrates more points near the leading edge, where the curvature is greatest, while fewer points are distributed near the trailing edge.
- (2) The  $x$ -coordinates are defined using angles ranging from 0 to  $\pi$ . This method distributes points symmetrically, ensuring equal point density near both the leading edge and trailing edge. However, the points near the mid-chord region are more sparsely distributed compared to the edge regions.

Since 1000 points are sufficient to produce a smooth graphical representation, both cosine spacing methods yield nearly identical results. In this study, the first method is adopted.

## Airfoil Graphing

For geometry-based thickness distributions, including the NACA 4-digit, 5-digit, and their modified series, the airfoil geometries are constructed using the analytical equations provided in the official NACA reports.

However, for airfoils designed based on thin airfoil theory, no explicit analytical thickness distributions are defined. Due to the complexity of aerodynamic analysis and the requirement for advanced computational tools, these airfoils are generated using available airfoil coordinate data. The governing equations are then approximated using Lagrange interpolation.

The geometric characteristics of airfoils vary significantly depending on changes in key parameters. These geometric variations directly influence aerodynamic performance, particularly lift, drag, and moment coefficients during flight.

In this study, one geometric parameter of a given NACA airfoil is varied while all other parameters are held constant. This approach allows for a clear observation of how individual parameters affect the airfoil shape.

## Numerical Accuracy Assessment

### Scope of the Error Analysis

The present tool does not involve CFD or flow-field simulation. The geometry is generated from analytical NACA formulations and, in some cases, reconstructed from tabulated coordinate data using polynomial interpolation.

Therefore, the primary sources of numerical error arise from:

- Discretization error due to finite chordwise sampling,
- Interpolation error from polynomial reconstruction,
- Tabulated data approximation and rounding.

Since the analytical NACA equations are available, they are treated as the reference solution for validation purposes.

### Discretization Error

Let  $y_{exact}(x)$  denote the analytical airfoil surface and  $y_N(x)$  the discretized representation using  $N$  chordwise points.

The discretization error is evaluated using:

$$E_\infty(N) = \max_i |y_N(x_i) - y_{exact}(x_i)| \quad (12)$$

and the root-mean-square (RMS) error:

$$E_{RMS}(N) = \sqrt{\frac{1}{N} \sum_{i=1}^N (y_N(x_i) - y_{exact}(x_i))^2} \quad (13)$$

A grid refinement study is performed by increasing  $N = 50, 100, 200$ .

For smooth analytical airfoil functions, the discretization error is expected to decrease approximately with  $\mathcal{O}(N^{-2})$  for sufficiently smooth regions.

## Effect of Node Distribution

Uniform spacing and cosine spacing are compared under identical  $N$ .

Since airfoil curvature is highest near the leading edge, uniform spacing under-resolves this region, leading to locally amplified error.

Cosine spacing clusters nodes near  $x = 0$ , thus significantly reducing leading-edge geometric error. For typical NACA 4-digit profiles, the maximum geometric deviation near the leading edge is expected to decrease by one order of magnitude when cosine spacing is used instead of uniform spacing at moderate resolution ( $N \approx 100$ ).

## Interpolation Error

When reconstructing geometry from tabulated data, Lagrange polynomial interpolation of degree  $n$  is applied.

The interpolation error is theoretically given by:

$$f(x) - P_n(x) = \frac{f^{(n+1)}(\xi)}{(n+1)!} \prod_{i=0}^n (x - x_i) \quad (14)$$

for some  $\xi$  in the interpolation interval.

Since airfoil thickness and camber distributions are smooth functions, the interpolation error remains small for moderate  $n$ . However, high-degree interpolation under uniform spacing may produce oscillations (Runge phenomenon).

In practical implementation, interpolation is restricted to moderate polynomial degree or applied locally to avoid instability.

The expected interpolation error magnitude, for  $n \leq 10$  and smooth tabulated data, is typically below  $10^{-4}c$  in geometric coordinates.

## Tabulated Data Approximation

Tabulated airfoil data are usually rounded to 4–5 decimal places. This introduces a baseline numerical uncertainty on the order of:

$$E_{table} \sim 10^{-5}c \text{ to } 10^{-4}c \quad (15)$$

which represents the lower bound of achievable accuracy when reconstructing geometry from such data.

## Overall Expected Accuracy

Combining discretization and interpolation effects, the total geometric error may be estimated as:

$$E_{total} \approx E_{disc} + E_{interp} + E_{table} \quad (16)$$

For typical configurations with:

- $N \geq 100$  cosine-spaced nodes,
- Moderate interpolation degree,

the overall geometric deviation is expected to remain within:

$$E_{total} \leq 10^{-4}c \quad (17)$$

which corresponds to less than 0.01% of the chord length.

## Acceptable Error and Adjustment Criteria

Since the present tool is intended for geometric visualization, preliminary aerodynamic estimation, and educational or conceptual analysis, a geometric tolerance of:

$$E_{tol} = 10^{-4}c \quad (18)$$

is considered acceptable.

If the error exceeds this threshold, the following adjustments are recommended:

- Increase chordwise resolution  $N$ ,

- Use cosine spacing instead of uniform spacing,
- Reduce interpolation degree or switch to spline interpolation,
- Refine tabulated input precision.

## Conclusion

The dominant numerical error source in the present implementation is discretization near the leading edge. Cosine spacing effectively mitigates this issue.

Under typical settings, the geometric error remains sufficiently small for engineering-level preliminary airfoil analysis. Further refinement is only necessary if high-fidelity CFD or structural analysis is to be performed using the generated geometry.

# Effect of Geometric Parameters on Airfoil Shape

## NACA 4-Digit Airfoil

The NACA 4-digit series defines the airfoil geometry through three primary parameters: maximum camber  $M$ , camber position  $P$ , and maximum thickness  $TT$ . These parameters independently control camber line curvature and thickness distribution, thus directly influencing aerodynamic performance.

### Maximum Camber

Airfoil geometries are generated by varying the maximum camber parameter  $M$  in the range from 1% to 5% of the chord, while keeping other parameters constant.

Increasing camber increases the curvature of the mean camber line, which leads to:

- Higher lift coefficient at zero angle of attack,
- Increased slope of the lift curve in the linear region,
- More negative pitching moment about the quarter-chord,
- Greater asymmetry between upper and lower surfaces.

From thin airfoil theory, camber primarily shifts the lift curve upward without significantly altering its slope. However, excessive camber may increase pressure gradients and accelerate boundary layer separation, thereby affecting stall characteristics.

## Camber Position

The camber position parameter  $P$  determines the chordwise location of maximum camber.

Forward camber (smaller  $P$  values) produces:

- Stronger suction peak near the leading edge,
- Higher lift at low angles of attack,
- Larger negative pitching moment.

Aft camber (larger  $P$  values) shifts the aerodynamic loading rearward, which may:

- Reduce the magnitude of the pitching moment,
- Improve stall behavior,
- Provide smoother pressure recovery.

Thus, camber position plays a critical role in balancing lift generation and moment characteristics.

## Thickness

The thickness parameter  $TT$  is varied from 9% to 16% of the chord.

Increasing thickness results in:

- Greater structural stiffness,
- Higher maximum lift coefficient,
- Delayed stall in many configurations,
- Increased profile drag, especially at higher Reynolds numbers.

Thicker airfoils also exhibit larger leading-edge radius, which improves tolerance to angle-of-attack variations. However, excessive thickness may increase form drag and reduce high-speed efficiency.

## Comparison of Selected NACA 4-Digit Airfoils

### NACA 0012

The NACA 0012 is a symmetric airfoil with zero camber and 12% thickness. Its symmetry implies:

- $C_L = 0$  at zero angle of attack,
- Nearly zero quarter-chord pitching moment,
- Identical aerodynamic behavior for positive and negative angles.

It is widely used in control surfaces and stabilizers where predictable and balanced aerodynamic response is required.

### NACA 2412

The NACA 2412 has 2% camber located at 40% chord and 12% thickness. Compared to NACA 0012:

- Generates positive lift at zero angle,
- Exhibits a negative pitching moment,
- Provides improved low-speed performance.

It is commonly applied in light aircraft wings due to its favorable lift-to-drag characteristics at moderate Reynolds numbers.

### NACA 4415

The NACA 4415 increases camber to 4% and thickness to 15%. Relative to NACA 2412:

- Produces higher lift capability,
- Has stronger negative pitching moment,
- Offers improved maximum lift coefficient,
- May incur higher drag at cruise conditions.

This airfoil is more suitable for applications requiring strong low-speed lift, such as utility aircraft or UAV platforms.

## NACA 5-Digit Airfoil

The NACA 5-digit series introduces a more refined camber definition, based on a specified design lift coefficient. The camber line is derived from theoretical aerodynamic loading considerations rather than purely geometric definition.

### Design Lift Coefficient

The first digit of the 5-digit series relates to the design lift coefficient. Airfoils with higher design lift coefficient exhibit stronger camber curvature.

This parameter determines the lift level at which minimum pressure drag is achieved, thus optimizing performance around a specific operating condition.

### Camber Position

The second digit controls the location of maximum camber. Compared to 4-digit series, 5-digit airfoils generally place maximum camber further forward, which enhances lift capability while maintaining improved aerodynamic efficiency.

### Reflex Indication

The third digit specifies whether the camber line is normal or reflexed.

Reflexed camber lines are designed to reduce or eliminate negative pitching moment, making them suitable for tailless aircraft configurations. The upward curvature near the trailing edge counteracts nose-down pitching tendencies.

### Thickness

Thickness variation affects structural and aerodynamic characteristics in the same manner as in the 4-digit series, but combined with a more aerodynamically optimized camber line.

## Modified 4- and 5-Digit Series

Modified series introduce additional geometric flexibility.

### Leading-Edge Radius

Increasing leading-edge radius:

- Reduces sensitivity to angle-of-attack variations,

- Improves stall characteristics,
- Delays flow separation onset.

Sharper leading edges may reduce drag in specific regimes but are more prone to abrupt stall.

### **Position of Maximum Thickness**

Moving maximum thickness forward:

- Improves structural efficiency,
- Alters pressure recovery behavior,
- Influences drag divergence characteristics.

Aft thickness location may improve high-speed performance but can reduce structural efficiency.

### **NACA 6 and 6A Series**

The 6-series airfoils are designed to maintain laminar flow over a specified portion of the chord.

### **Design Lift Coefficient**

The design lift coefficient determines the lift level at which minimum drag occurs. The pressure distribution is tailored to produce a favorable pressure gradient over an extended chordwise region.

### **Thickness**

Thickness variation affects both structural capability and laminar flow stability. Excessive thickness may shorten laminar run length, while insufficient thickness compromises structural integrity.

The 6A series modifies camber definitions to improve pitching moment characteristics and expand practical operating envelopes.

# Practical Applications of NACA Airfoil Families

NACA airfoils have been widely used in aircraft, propellers, rotating machinery, and renewable energy systems. Each NACA series was developed with different aerodynamic objectives, and their geometric characteristics determine their suitability for specific engineering applications.

## NACA 4-Digit Series

The NACA 4-digit series is defined by maximum camber, camber position, and maximum thickness. Due to its simplicity and robustness, this family is among the most widely applied airfoil series in history.

### Symmetric 4-Digit Airfoils (NACA 00XX)

Examples: NACA 0009, NACA 0012, NACA 0015.

#### Geometric Characteristics

- Zero camber
- Symmetric upper and lower surfaces
- Moderate thickness (9%–15%)

#### Aerodynamic Characteristics

- Zero lift at zero angle of attack
- Nearly zero quarter-chord pitching moment
- Identical behavior for positive and negative angles

#### Applications

- Horizontal and vertical stabilizers
- Control surfaces (rudders, elevators)
- Aerobatic aircraft wings
- Helicopter rotor sections (in symmetric loading regions)
- Experimental and research wind tunnel models

For example, NACA 0012 has historically been used in stabilizer surfaces and as a benchmark airfoil in aerodynamic testing.

## Cambered 4-Digit Airfoils (e.g., NACA 2412, 4412)

### Geometric Characteristics

- Camber typically 2%–4%
- Camber position near 30%–40% chord
- Thickness commonly 12%

### Aerodynamic Characteristics

- Positive lift at zero angle of attack
- Improved low-speed performance
- Moderate negative pitching moment

### Applications

- General aviation aircraft wings
- Light trainer aircraft
- Small UAV platforms
- Model aircraft

The NACA 2412, for instance, has been used on several light aircraft designs due to its favorable lift-to-drag ratio at moderate Reynolds numbers ( $10^6$  range).

## NACA 5-Digit Series

The NACA 5-digit series was designed based on a specified design lift coefficient. It provides improved aerodynamic efficiency compared to the basic 4-digit series.

### Geometric Characteristics

- Camber defined from theoretical lift distribution
- Often stronger forward camber
- Option for reflex camber line

### Aerodynamic Characteristics

- Higher lift coefficient capability

- Optimized performance at a target lift condition
- Reduced pitching moment (in reflexed versions)

## **Applications**

- Early transport aircraft
- Aircraft requiring higher lift coefficients
- Tailless and flying-wing aircraft (reflex versions)

Reflexed 5-digit airfoils were particularly important in configurations where pitching moment control had to be minimized without a horizontal tail.

## **NACA 6-Series**

The NACA 6-series was developed to achieve extended laminar flow and reduce profile drag.

### **Geometric Characteristics**

- Carefully shaped pressure distribution
- Reduced suction peak
- Designed laminar flow region

### **Aerodynamic Characteristics**

- Low drag within a specified lift coefficient range
- High sensitivity to surface roughness
- Narrow optimal operating envelope

## **Applications**

- High-performance gliders
- Long-range propeller aircraft
- Endurance UAVs

For example, several 6-series airfoils were used in mid-20th century aircraft designed for improved cruise efficiency.

## **NACA 6A-Series**

The 6A-series is a modification of the 6-series, improving pitching moment behavior and broadening operational stability.

### **Applications**

- Military trainer aircraft
- Aircraft requiring better handling characteristics

These airfoils offered improved practicality compared to the original 6-series designs.

## **Applications in Rotating Machinery**

### **Propellers and Helicopter Rotors**

NACA airfoils are frequently used as sectional profiles along rotating blades.

- Thicker sections near the root for structural strength
- Thinner or more efficient sections near the tip
- Cambered profiles to increase thrust generation

Typical Reynolds numbers vary significantly along the span, requiring careful airfoil selection.

### **Axial Fans and Compressors**

Early-stage axial fans and low-speed compressors often used NACA-derived airfoil shapes for predictable pressure rise and manageable stall behavior.

Design considerations include:

- Pressure gradient tolerance
- Flow turning capability
- Structural thickness for centrifugal loading

## Wind Turbines

In small-scale wind turbines, NACA 4-digit airfoils are commonly used for simplicity and well-documented performance.

- Thick sections near blade root
- Higher lift-to-drag ratio sections toward mid-span
- Cambered profiles for improved energy extraction

Modern large turbines often employ specialized airfoils, but NACA geometries remain useful for preliminary design and educational studies.

## Summary of Engineering Usage

In summary:

- NACA 00XX: stabilizers, control surfaces, symmetric loading.
- Cambered 4-digit: general aviation and small UAV wings.
- 5-digit: higher lift and optimized cruise performance.
- Reflex 5-digit: tailless aircraft.
- 6-series: laminar-flow cruise optimization.
- Modified or thick variants: rotating machinery and wind turbines.

The broad applicability of NACA airfoils stems from their parametric geometric structure, which enables systematic adaptation to diverse aerodynamic and structural requirements.

## Results and Conclusion

### Excel model capabilities

### Assessment

This study summarizes the evolution of NACA airfoils, from early geometry-based definitions to modern aerodynamic and empirical design approaches. Initially, airfoil design relied primarily on geometric parameters such as camber, camber position, and thickness, which allowed engineers to generate airfoil shapes using analytical

equations. These early methods provided a foundation for understanding airfoil geometry and its influence on aerodynamic performance.

However, with the advancement of aerodynamic theory and computational tools, airfoil design has gradually shifted toward performance-based approaches. Modern airfoil development focuses on achieving specific aerodynamic objectives, such as target lift coefficients, favorable pressure distributions, and improved lift-to-drag ratios.

Simulation also plays a critical role in airfoil analysis, although numerical results may contain errors due to discretization, interpolation, numerical approximation, and modeling assumptions. Therefore, simulation results must be carefully validated and interpreted.

In practical applications, the digits in NACA series are not strictly followed during manufacturing. Although airfoils may retain their NACA designation, their geometries are often refined through aerodynamic analysis, numerical simulations, and experimental validation. These refinements ensure that the final airfoil meets performance, stability, and efficiency requirements for specific applications such as aircraft wings, propellers, or turbine blades.

## Discussion

### Classical Design Approach

The classical airfoil design approach was primarily theoretical and geometry-driven. Engineers defined airfoil shapes using analytical equations without detailed aerodynamic performance predictions. The aerodynamic characteristics were then evaluated through experiments and empirical observations, followed by iterative modifications.

Although this approach established important theoretical foundations and provided valuable design concepts, it often resulted in inefficient designs and a relatively high failure ratio. The lack of accurate predictive tools made it difficult to optimize airfoils for specific aerodynamic requirements.

### Modern Design Approach

Modern airfoil design relies heavily on numerical methods and computational tools. Airfoils are now designed to meet specific aerodynamic performance targets, such as desired lift coefficients  $C_l$ , lift-to-drag ratios, and pressure or velocity distributions along the chord.

The modern design process typically follows these steps:

- Define aerodynamic performance requirements

- Generate airfoil geometry using numerical optimization methods
- Simulate aerodynamic performance using computational tools
- Manufacture prototypes
- Conduct experimental validation
- Refine and optimize the design based on results

This approach significantly improves design reliability, efficiency, and performance compared to classical methods.

Modern airfoils are no longer defined solely by geometric parameters, but by aerodynamic performance objectives. The development of computational fluid dynamics (CFD) and numerical optimization allows engineers to design airfoils with precise aerodynamic characteristics.

## **Limitations of 2D Airfoil Analysis and Transition to 3D Design**

Airfoil sections represent only a two-dimensional approximation of wing behavior. The aerodynamic characteristics of a 2D airfoil correspond to those of an infinite wing with infinite aspect ratio, which does not exist in practical applications.

In reality, wings, propeller blades, and turbine blades are three-dimensional and finite structures. Their aerodynamic behavior is influenced by additional factors such as wingtip vortices, induced drag, and spanwise flow. As a result, accurate aerodynamic analysis requires three-dimensional numerical simulations.

Fortunately, modern aerospace engineering provides advanced computational tools such as OpenFOAM, OpenVSP, and ANSYS, which enable engineers to perform detailed aerodynamic simulations and optimize designs efficiently.

The development of such tools reflects the interdisciplinary nature of modern aerospace engineering. Their creation requires expertise in aerodynamics, applied mathematics, numerical methods, and computer science. This interdisciplinary collaboration has significantly improved the accuracy, efficiency, and reliability of airfoil and aircraft design.

# Appendix

## Cosine Spacing and Half-Cosine Spacing

### Motivation

In airfoil geometry discretization, a uniform spacing in the chordwise direction often fails to accurately capture regions with high curvature, especially near the leading edge. Since the leading edge radius is small and the curvature is large, clustering points in this region improves geometric resolution and numerical stability.

To achieve non-uniform but smoothly distributed points, cosine-based spacing techniques are commonly used.

### Cosine Spacing

Let the chord length be normalized such that  $x \in [0, 1]$ . We introduce an auxiliary angular parameter:

$$\theta \in [0, \pi] \quad (19)$$

The cosine spacing transformation is defined as:

$$x(\theta) = \frac{1}{2}(1 - \cos \theta) \quad (20)$$

If  $N$  points are required, we define:

$$\theta_i = \frac{i\pi}{N-1}, \quad i = 0, 1, \dots, N-1 \quad (21)$$

Thus,

$$x_i = \frac{1}{2} \left( 1 - \cos \frac{i\pi}{N-1} \right) \quad (22)$$

### Properties

- Point clustering occurs near both  $x = 0$  (leading edge) and  $x = 1$  (trailing edge).
- The distribution is symmetric with respect to  $x = 0.5$ .
- The spacing density follows the derivative:

$$\frac{dx}{d\theta} = \frac{1}{2} \sin \theta \quad (23)$$

Since  $\sin \theta \rightarrow 0$  as  $\theta \rightarrow 0$  and  $\theta \rightarrow \pi$ , the spacing becomes denser near the endpoints.

### Half-Cosine Spacing

In some applications, clustering is only required near the leading edge. In this case, the half-cosine transformation is used:

$$\theta \in [0, \frac{\pi}{2}] \quad (24)$$

$$x(\theta) = 1 - \cos \theta \quad (25)$$

For  $N$  points:

$$\theta_i = \frac{i}{N-1} \cdot \frac{\pi}{2}, \quad i = 0, 1, \dots, N-1 \quad (26)$$

$$x_i = 1 - \cos \left( \frac{i}{N-1} \cdot \frac{\pi}{2} \right) \quad (27)$$

Characteristics

- Strong clustering near  $x = 0$ .
- Nearly uniform spacing toward  $x = 1$ .
- Particularly suitable for airfoil leading edge refinement.

### Comparison with Uniform Spacing

For reference, uniform spacing is defined as:

$$x_i = \frac{i}{N-1} \quad (28)$$

Uniform spacing does not account for geometric curvature and may require a significantly larger number of points to achieve comparable leading-edge accuracy.

Cosine-based spacing provides higher geometric resolution with the same number of discretization points.

## Lagrange Interpolation

### Definition

Given a set of  $n + 1$  distinct data points:

$$(x_0, y_0), (x_1, y_1), \dots, (x_n, y_n) \quad (29)$$

the Lagrange interpolation polynomial  $P_n(x)$  of degree at most  $n$  is defined as:

$$P_n(x) = \sum_{j=0}^n y_j L_j(x) \quad (30)$$

where  $L_j(x)$  are the Lagrange basis polynomials:

$$L_j(x) = \prod_{\substack{m=0 \\ m \neq j}}^n \frac{x - x_m}{x_j - x_m} \quad (31)$$

### Interpolation Property

The basis polynomials satisfy:

$$L_j(x_i) = \begin{cases} 1, & i = j \\ 0, & i \neq j \end{cases} \quad (32)$$

Thus,

$$P_n(x_i) = y_i \quad (33)$$

which guarantees exact interpolation at the given nodes.

### Application in Airfoil Geometry

In airfoil reconstruction, Lagrange interpolation can be used to:

- Interpolate discrete airfoil coordinate data.
- Construct smooth curves from control points.
- Approximate camber line or thickness distribution functions.

However, for large  $n$ , high-degree interpolation may suffer from Runge's phenomenon, especially under uniform spacing. Using cosine-spaced nodes significantly improves numerical stability.

### Error Estimation

The interpolation error is given by:

$$f(x) - P_n(x) = \frac{f^{(n+1)}(\xi)}{(n+1)!} \prod_{i=0}^n (x - x_i) \quad (34)$$

for some  $\xi$  in the interval containing the nodes.

This expression shows that:

- The error depends on node placement.
- Clustering nodes (e.g., cosine spacing) reduces oscillatory behavior.

# References

- [1] Jr. Charles L.Ladson, Cuyler W.Brooks. Developement of a computer program to obtain ordinats for naca 4-digit, 4-digit modified, 5-digit, and 16-series airfoils. *National Aeronautics ans Space Administration (NACA)*, November 1975.
- [2] Kenneth E.Ward Eastman N.Jacobs and Robert M.Pinkerton. The characteristics of 78 related airfoils sections from tests in the variable-density wind tunnel. *Langley Memorial Aeronautical Laboratory, National Advisory Committee for Aeronautics, National Advisory Commitee for Aeronautics, Langley Field*, December 20, 1932.
- [3] Louis S.Stivers Jr. Ira H.Abbott, Albert E.von Doenhoff. Summary of airfoil data. *National Advisory Commitee for Aeronautics (NACA)*, 1935.
- [4] Eastman N.Jacob and Robert M.Pinkerton. The variable-density wind tunnel of related airfoils having the maximum camber unusually far forward. *Langley Memorial Aeronautical Laboratory, National Advisory Committee for Aeronau-tics, National Advisory Commitee for Aeronautics, Langley Field*, May 7, 1935.
- [5] Alan Pope. Basic wing and airfoil theory. *McGrall-Hill book Company, Inc*, 1951.
- [6] John Stack and Albert E.Von Doenhoff. Tets of 16 related airfoils at high speeds. *Langley Memorial Aeronautical Laboratory, National Advisory Committee for Aeronautics, National Advisory Commitee for Aeronautics, Langley Field*, April 28, 1934.